Astronomy & Astrophysics

X-ray variability of Pleiades late-type stars as observed with the ROSAT-PSPC

A. Marino[1], G. Micela[2], G. Peres[1], and S. Sciortino[2]

[1] Dipartimento di Scienze Fisiche e Astronomiche, Sez. di Astronomia, Università di Palermo, Piazza del Parlamento 1, 90134 Palermo, Italy
e-mail: marino@oapa.astropa.unipa.it; peres@oapa.astropa.unipa.it

[2] INAF – Osservatorio Astronomico di Palermo G.S. Vaiana, Piazza del Parlamento 1, 90134 Palermo, Italy
e-mail: giusi@oapa.astropa.unipa.it, sciorti@oapa.astropa.unipa.it

Abstract. We present a comprehensive analysis of X-ray variability of the late-type (dF7-dM) Pleiades stars, detected in all ROSAT-PSPC observations; X-ray variations on short (hours) and medium (months) time scales have been explored. We have grouped the stars in two samples: 89 observations of 42 distinct dF7-dK2 stars and 108 observations of 61 dK3-dM stars.

The Kolmogorov-Smirnov test applied on all X-ray photon time series show that the percentage of cases of significant variability is quite similar on both samples, suggesting that the presence of variability does not depend on mass for the time scales and mass range explored.

The comparison between the Time X-ray Amplitude Distribution functions (XAD) of the set of dF7-dK2 and of the dK3-dM show that, on short time scales, dK3-dM stars show larger variations than dF7-dK2.

A subsample of eleven dF7-dK2 and eleven dK3-dM Pleiades stars allows the study of variability on longer time scales: we found that variability on medium – long time scales is relatively more common among dF7-dK2 stars than among dK3-dM ones. For both dF7-dK2 Pleiades stars and dF7-dK2 field stars, the variability on short time scales depends on L_x while this dependence has not been observed among dK3-dM stars. It may be that the variability among dK3-dM stars is dominated by flares that have a similar luminosity distribution for stars of different L_x, while flaring distribution in dF7-dK2 stars may depend on X-ray luminosity. The lowest mass stars show significant rapid variability (flares?) and no evidence of rotation modulation or cycles. On the contrary, dF7-dK2 Pleiades stars show both rapid variability and variations on longer time scales, likely associated with rotational modulation or cycles.

Key words. open clusters and associations: individual: Pleiades – stars: coronae – stars: late-type – stars: rotation – X-ray: stars

1. Introduction

Because of its closeness, the Sun is the only star for which X-ray variability is extensively studied on all time scales (e.g. Vaiana et al. 1973; Vaiana & Tucker 1974; Kreplin et al. 1977; Withbroe et al. 1985). The Sun exhibits large variability in X-rays with amplitudes of more than one order of magnitude due to flares, rotational modulation and the 11-year cycle. Moreover, observations of the Sun have high spatial, spectral and temporal resolution, and span a much longer time interval than stellar observations. Resolving the structure of the solar corona (presently down to ~700 km) allows us to identify directly the sources of X-ray emission and to relate variations of the global solar X-ray flux (e.g. Kreplin et al. 1977; Kahler & Kreplin 1991; Peres et al. 2000; Orlando et al. 2001) to the originating structures on the Sun.

Since no equivalent studies are possible for other stars, variability studies of homogeneous classes of stars provide a powerful tool to study coronal emitters and to constrain the X-ray generating mechanisms.

In this perspective we have analyzed the X-ray variability properties of nearby dK3-dM and of dF7-dK2 stars as observed with ROSAT-PSPC (Marino et al. 2000, 2002, hereafter Paper I and Paper II).

The systematic analysis of nearby dK3-dM stars (Paper I) showed that X-ray variability is a general property of these stars on all time scales explored. The amplitude of these variations is independent of both stellar X-ray and visual luminosity. Compared to properties of solar X-ray variability, our results suggest that the amplitude distribution of X-ray variations of dK3-dM stars is consistent with the analogous distribution for solar flares. The comparison of ROSAT-PSPC data with those obtained with *Einstein IPC* has showed that long term variability (i.e. on time scales longer than 10 years), if present, must be

Table 1. ROSAT-PSPC observations of the Pleiades.

Obs. id.	Obs. seq.	Elapsed time (ks)	Start date	End date
1	rp200008a00	2022.822	9-Feb.-91	4-Mar.-91
2	rp200068a00	1984.662	9-Feb.-91	4-Mar.-91
3	rp200008a01	80.081	21-Aug.-91	22-Aug.-91
4	rp200068a01	86.143	22-Aug.-91	23-Aug.-91
5	rp200556n00	71.185	6-Sep.-91	7-Sep.-91
6	rp200557n00	82.704	5-Sep.-91	6-Sep.-91
7	rp200008a02	185.855	27-Aug.-92	29-Aug.-92

of smaller amplitude than the short term variations observed in the ROSAT X-ray light curves.

The analysis of dF7-dK2 stars in the solar neighborhood showed that the amplitude of their X-ray variability is smaller than that observed in nearby dK3-dM stars. For a subsample observed both at the beginning and at the end of the mission, we studied the variability on time scale of years and compared amplitude variations at short and long time scales; for these stars, the X-ray variability is more significant on the longer time scale. Furthermore all the stars variable on the long time scale, and not on the short time scale, are relatively quiet and similar to the Sun, suggesting that the variations may be due to cycles.

Open clusters are ideal samples to study evolutionary effects to complete our picture. Furthermore, in a given cluster, the distance and other stellar parameters such as age and metallicity are approximately fixed and it is possible to study how the coronal emission properties change with mass.

In particular the Pleiades was one of the primary open clusters observed and studied because of its youth and proximity (e.g. Caillault & Helfand 1985; Micela et al. 1985, 1990; Schmitt et al. 1993; Stauffer et al. 1994; Gagné et al. 1995; Micela et al. 1996, 1999; Krishnamurthi et al. 2001; Daniel et al. 2002)

Temporal analyzes of Pleiades X-ray data, using single ROSAT observations, have been made by Schmitt et al. (1993), Stauffer et al. (1994), and Micela et al. (1996). Schmitt et al. (1993), comparing ROSAT All Sky Survey data with Einstein/IPC data, suggested that the observed variability on ten year time scales may be evidence for a solar-like cyclic activity. Micela et al. (1996) find that most of the Pleiades stars show variability within a factor two-three, both on six month and, using Einstein observations, on ten year time scales, while the few stars with evidence of larger variations show large flares on shorter time scales. Gagné et al. (1995) find that on ~1 yr timescales, approximately 25% of the late-type Pleiades stars are variable by more than a factor 2, while they find only a marginal evidence for increased variability on the 10 yr timescale. The magnitude and the frequency of variations in the stars of the Pleiades's core region, observed with Chandra, are consistent with the results found by Schmitt et al. (1993) and Daniel et al. (2002).

In this paper we present a study of X-ray variability of late-type Pleiades stars analyzing all pointed observations of

ROSAT-PSPC. We explore X-ray variability properties on short (hours), and medium (months) time scales, and we compare our data with those obtained for late-type field stars.

Our paper is organized as follows: in Sect. 2 we present our sample of dF7-dK2 and dK3-dM Pleiades stars, the X-ray data, and their analysis; the results are given in Sect. 3; in Sect. 4, we discuss them and draw our conclusions.

2. PSPC observations and data analysis

2.1. The sample

The Pleiades catalog employed in this study has been selected by Prosser and Stauffer as part of the Open Cluster Database project, available at `http://cfa-www.harvard.edu/stauffer`

We selected and grouped the stars having a de-reddened $(B-V)_0$ color between 0.5 and 0.9 (spectral type dF7-dK2), and those having $(B-V)_0 > 0.9$ (spectral type dK3-dM), detected with more than 40 net counts and at an off-axis angle from the center of the field of view ≤48 arcmin, as described in the next section.

The dF7-dK2 sample consists of 42 stars, for a total of 89 distinct observations. The dK3-dM sample consists of 61 stars, for a total of 108 distinct observations.

A few stars were multiply observed with ROSAT-PSPC at time intervals typically of a few months; in these cases we can explore variability up to these time scales.

2.2. X-ray observations

We used data from seven ROSAT-PSPC pointed observations of the Pleiades. The characteristics of the observations are summarized in Table 1. The progressive number in Col. 1 is a reference for Tables 2 and 3. Column 2 gives the ROSAT Observation Request (ROR) and Col. 3 the total time spanned by the observations. The start and the end date of the observations are listed in Cols. 4 and 5.

Tables 2 and 3 provide the characteristics of ROSAT-PSPC detected stars. Column 1 gives the star's name, Col. 2 identifies the PSPC field (Col. 1 in Table 1). Column 3 yields the effective exposure-time for each detection, Col. 4 gives the count rate, Col. 5 the mean X-ray luminosity and Col. 6 the results of the Kolmogorov-Smirnov test (e.g. Eadie et al. 1971; Siegel 1956), discussed in Sect. 3.

Table 2. ROSAT PSPC detections of dF7-dK2 Pleiades stars.

Name	Obs. id.	Exposure time (s)	Rate ± err. [10^{-2} cnt/s]	$\log L_x$ ± err. [erg/s]	CL range for variability
HII-174	6	23 413.85	7.30 ± 0.20	30.05 ± 0.03	≥99%
HII-193	6	20 108.73	0.80 ± 0.10	29.10 ± 0.05	90%–95%
HII-250	6	24 628.54	1.00 ± 0.10	29.18 ± 0.05	≤90%
HII-253	3	13 022.5	8.40 ± 0.30	30.11 ± 0.03	95%–99%
HII-253	7	4170.27	4.90 ± 0.30	29.87 ± 0.05	≤90%
HII-253	6	24 052.5	12.30 ± 0.20	30.27 ± 0.03	≥99%
HII-263	6	20 635.51	1.80 ± 0.10	29.45 ± 0.04	≤90%
HII-345	6	25 516.8	6.30 ± 0.20	29.98 ± 0.03	≥99%
HII-405	6	25 889.14	2.00 ± 0.10	29.48 ± 0.04	≤90%
HII-476	3	16 482.96	1.40 ± 0.10	29.32 ± 0.05	95%–99%
HII-476	4	20 770.20	0.90 ± 0.10	29.13 ± 0.05	≥99%
HII-514	6	20 076.17	0.32 ± 0.04	28.68 ± 0.07	≤90%
HII-625	2	8427.67	2.00 ± 0.20	29.48 ± 0.05	≥99%
HII-627	6	23 906.4	1.30 ± 0.10	29.31 ± 0.04	≤90%
HII-708	3	13 433.22	3.40 ± 0.20	29.72 ± 0.04	≥99%
HII-708	7	4251.17	2.80 ± 0.30	29.63 ± 0.06	95%–99%
HII-708	6	16 233.41	0.40 ± 0.10	28.82 ± 0.07	≤90%
HII-727	1	3438.85	4.00 ± 0.30	29.79 ± 0.06	≥99%
HII-727	3	16 203.27	4.30 ± 0.20	29.81 ± 0.04	90%–95%
HII-727	4	14 892.66	4.40 ± 0.20	29.83 ± 0.04	≤90%
HII-727	7	4876.28	3.60 ± 0.30	29.75 ± 0.05	≤90%
HII-738	4	23 533.99	3.30 ± 0.10	29.70 ± 0.04	95%–99%
HII-738	2	9970.83	3.20 ± 0.20	29.69 ± 0.04	≥99%
HII-738	7	4632.96	2.50 ± 0.20	29.58 ± 0.06	≤90%
HII-745	7	4906.33	1.30 ± 0.20	29.31 ± 0.07	≤90%
HII-746	4	18 562.4	0.80 ± 0.10	29.09 ± 0.06	≤90%
HII-761	1	4495.5	2.10 ± 0.20	29.51 ± 0.06	≥99%
HII-761	3	18 535.14	3.50 ± 0.10	29.73 ± 0.04	≤90%
HII-761	7	5595.73	3.10 ± 0.20	29.68 ± 0.05	95%–99%
HII-761	2	7994.81	3.20 ± 0.20	29.69 ± 0.05	≥99%
HII-761	4	21 951.15	3.00 ± 0.10	29.66 ± 0.04	≤90%
HII-761	6	18 306.31	2.80 ± 0.10	29.62 ± 0.04	≤90%
HII-870	4	24 701.33	0.21 ± 0.03	28.51 ± 0.08	≤90%
HII-923	2	8388.73	2.30 ± 0.20	29.54 ± 0.05	≥99%
HII-923	4	18 561.54	2.80 ± 0.10	29.63 ± 0.04	≥99%
HII-975	4	21 291.28	0.60 ± 0.10	28.99 ± 0.06	≤90%
HII-996	6	21 552.99	1.60 ± 0.10	29.39 ± 0.04	≤90%
HII-1015	6	18 001.6	0.80 ± 0.10	29.09 ± 0.06	≤90%
HII-1032	1	4397.89	4.70 ± 0.30	29.86 ± 0.05	≥99%
HII-1032	3	19 737	7.10 ± 0.20	30.04 ± 0.03	≥99%
HII-1032	7	5319.43	6.00 ± 0.30	29.96 ± 0.04	90%–95%
HII-1032	2	7937.35	4.10 ± 0.20	29.80 ± 0.04	≥99%
HII-1032	4	19 279.31	7.40 ± 0.20	30.06 ± 0.03	≥99%
HII-1032	6	17 681.85	6.50 ± 0.20	29.99 ± 0.03	≤90%
HII-1039	4	23 442.89	1.40 ± 0.10	29.32 ± 0.04	≤90%
HII-1039	2	8662.81	0.70 ± 0.10	29.05 ± 0.07	≥99%
HII-1039	3	15 978.54	1.00 ± 0.10	29.17 ± 0.06	90%–95%
HII-1117	3	18 056.79	0.90 ± 0.10	29.16 ± 0.05	90%–95%
HII-1117	2	11 444.06	1.10 ± 0.10	29.23 ± 0.06	≥99%
HII-1117	4	25 133.86	1.00 ± 0.10	29.17 ± 0.05	≤90%
HII-1124	4	25 018.06	1.30 ± 0.10	29.30 ± 0.04	90%–95%
HII-1124	3	20 609.86	1.20 ± 0.10	29.26 ± 0.05	95%–99%
HII-1124	2	11 378.28	1.40 ± 0.10	29.33 ± 0.05	≥99%
HII-1124	1	5285.27	1.10 ± 0.10	29.23 ± 0.08	≥99%
HII-1124	7	6466.06	1.30 ± 0.10	29.29 ± 0.07	≤90%
HII-1136	4	21 801.3	3.90 ± 0.10	29.78 ± 0.04	≤90%
HII-1136	2	8224.66	3.90 ± 0.20	29.77 ± 0.04	≥99%
HII-1136	3	13 709.38	2.90 ± 0.10	29.64 ± 0.04	≥99%
HII-1136	7	4279.33	2.30 ± 0.20	29.54 ± 0.06	≤90%
HII-1207	3	14 826	0.60 ± 0.10	28.97 ± 0.07	≤90%

Table 2. continued.

Name	Obs. id.	Exposure time (s)	Rate ± err. [10^{-2} cnt/s]	$\log L_x$ ± err. [erg/s]	CL range for variability
HII-1207	6	18 008.28	1.90 ± 0.10	29.47 ± 0.04	≤90%
HII-1215	4	20 461.12	1.10 ± 0.10	29.24 ± 0.05	≤90%
HII-1514	3	18 350.56	0.90 ± 0.10	29.12 ± 0.05	≤90%
HII-1514	7	5890.11	0.80 ± 0.10	29.10 ± 0.08	≤90%
HII-1514	4	18 765.89	0.70 ± 0.10	29.04 ± 0.06	≤90%
HII-1514	5	16 165.96	1.40 ± 0.10	29.32 ± 0.05	≥99%
HII-1613	3	17 908.14	0.90 ± 0.10	29.12 ± 0.06	≤90%
HII-1613	2	10 228.28	0.70 ± 0.10	29.03 ± 0.07	≥99%
HII-1613	4	23 234.28	1.10 ± 0.10	29.21 ± 0.05	≤90%
HII-1645	4	19 528.78	0.80 ± 0.10	29.11 ± 0.05	≥99%
HII-1726	1	4241.35	1.10 ± 0.20	29.21 ± 0.09	≥99%
HII-1726	3	18 107.51	1.50 ± 0.10	29.35 ± 0.05	≤90%
HII-1726	7	5358.72	1.90 ± 0.20	29.46 ± 0.06	≤90%
HII-1726	2	9559.15	1.10 ± 0.10	29.23 ± 0.06	95%–99%
HII-1726	4	21 312.57	130 ± 0.10	29.31 ± 0.05	≤90%
HII-1726	5	17 439.17	1.10 ± 0.10	29.23 ± 0.05	≤90%
HII-1797	4	20 773.6	2.80 ± 0.10	29.64 ± 0.04	≥99%
HII-1856	2	9854.4	1.00 ± 0.10	29.18 ± 0.06	90%–95%
HII-1856	4	20 972.84	1.80 ± 0.10	29.43 ± 0.04	≤90%
HII-1924	4	17 407.83	0.50 ± 0.10	28.86 ± 0.07	95%–99%
HII-2027	5	14 904.86	1.40 ± 0.10	29.34 ± 0.05	≥99%
HII-2147	3	14 708.35	16.10 ± 0.30	30.39 ± 0.03	≥99%
HII-2147	2	8812.89	9.90 ± 0.30	30.18 ± 0.03	≥99%
HII-2147	4	18 564.1	15.70 ± 0.30	30.38 ± 0.03	≥99%
HII-2147	5	15 113.59	15.20 ± 0.30	30.37 ± 0.03	≥99%
HII-2172	5	15 292.01	0.90 ± 0.10	29.14 ± 0.06	≤90%
HII-2644	5	20 302.72	0.40 ± 0.04	28.78 ± 0.07	≥99%
HII-2880	5	19 676.55	0.42 ± 0.05	28.81 ± 0.07	≤90%
HII-2881	5	14 457.12	3.40 ± 0.20	29.72 ± 0.04	≥99%

For each star we evaluated the photon counts in a circular region centered on the average position of the photons in the (0.1–2.4) keV range; the radius R ranges from 1 arcmin for sources on the optical axis, up to 4 arcmin, for sources at large off-axis positions; it has been determined as described in Paper I. Count rates of the off-axis sources were corrected for vignetting.

The background was measured in an annulus, between R+25 arcsec and R+50 arcsec, centered on the centroid of the source. If the source is in crowded areas we had to do "pie cuts" of the background annulus in order to avoid contributions from nearby sources. We excluded the sources near the window support structures of the PSPC and the ones in too crowded regions.

2.3. Count rate, flux and luminosity determination

The count rate in the 0.11–2.4 keV passband has been evaluated by dividing the net source counts by the effective time (Col. 3 of Tables 2 and 3) computed from the exposure map at the source position. We converted the count rates to flux in the 0.11–2.4 keV energy band, using a constant conversion factor of 9.47×10^{-12} erg cm^{-2}/count, obtained assuming a source

temperature of $\sim 7 \times 10^6$ K and a hydrogen column density of $N_{\rm H} = 10^{20.3}$ cm^{-2} (Bohlin et al. 1978). The estimated overall uncertainty of this conversion factor is of the order of 15%. X-ray luminosities were computed assuming a common distance of 116 pc taken from Hipparcos observations (Mermilliod et al. 1997).

Each observation consists of a set of temporal segments typically obtained during different satellite orbits; we estimated count rate, flux and X-ray luminosity for each temporal segment where at least 30 net source counts have been collected.

3. Results

3.1. Time variability

The analysis of all observations of the Pleiades, obtained with the ROSAT-PSPC mission, allows us to explore the X-ray variability on time scales that range from a few hours to 18 months.

For each star in our sample, we obtained light curves in the (0.11–2.4) keV band.

As in Paper I, we applied the unbinned Kolmogorov-Smirnov (K-S) test[1] to all X-ray photon time series of

---

[1] As implemented with pros.xtiming package within IRAF.

Table 3. ROSAT PSPC detections of dK3-dM Pleiades stars.

Name	Obs. id.	Exposure Time (s)	Rate ± err. [10^{-2} cnt/s]	$\log L_x$ ± err. [erg/s]	CL range for variability
AK-1B121	6	14 331.65	5.10 ± 0.20	29.89 ± 0.04	≤90%
HCG-65	6	18 954.15	1.50 ± 0.10	29.36 ± 0.05	≤90%
HCG-97	6	21 101.35	1.30 ± 0.10	29.31 ± 0.05	≥99%
HII-97	6	19 079.37	1.30 ± 0.10	29.3 ± 0.05	95%–99%
HCG-109	6	24 307.12	0.31 ± 0.04	28.67 ± 0.07	≤90%
HCG-123	6	24 265.38	0.80 ± 0.10	29.09 ± 0.05	95%–99%
HII-133	6	18 975.85	1.60 ± 0.10	29.39 ± 0.05	≥99%
HCG-134	6	20 572.90	0.60 ± 0.10	28.99 ± 0.06	≤90%
HII-134	6	19 556.06	0.80 ± 0.10	29.08 ± 0.06	≤90%
HCG-143	6	19 051.82	1.50 ± 0.10	29.36 ± 0.05	≥99%
HCG-144	4	20 075.41	4.70 ± 0.20	29.85 ± 0.03	≥99%
HCG-148	6	26 304.05	0.23 ± 0.03	28.54 ± 0.08	≥99%
HCG-172	6	25 050.13	0.34 ± 0.04	28.72 ± 0.07	≥99%
HII-191	6	25 913.35	1.00 ± 0.10	29.20 ± 0.05	≥99%
HII-212	6	21 391.87	1.10 ± 0.10	29.24 ± 0.05	≥99%
HCG-219	3	20 934.63	0.40 ± 0.04	28.78 ± 0.07	90%–95%
HCG-219	4	22 956.71	0.39 ± 0.04	28.78 ± 0.07	≤90%
HCG-219	7	6697.19	1.00 ± 0.10	29.16 ± 0.07	≥99%
HCG-244	3	20 058.24	0.70 ± 0.10	29.02 ± 0.06	≤90%
HCG-244	4	21 782.57	0.49 ± 0.05	28.87 ± 0.06	≤90%
HCG-244	7	6652.85	0.70 ± 0.10	29.02 ± 0.08	≤90%
HCG-246	1	4427.1	1.60 ± 0.20	29.38 ± 0.07	≥99%
HCG-258	4	25 729.02	0.64 ± 0.05	28.99 ± 0.05	95%–99%
HCG-258	2	11 561.63	1.00 ± 0.10	29.18 ± 0.06	≥99%
HCG-269	4	22 725.12	0.60 ± 0.10	28.96 ± 0.06	≤90%
HCG-273	3	19 038.85	1.20 ± 0.10	29.26 ± 0.05	≥99%
HCG-277	4	24 605.96	0.70 ± 0.10	29.02 ± 0.05	≤90%
HCG-277	2	9462.75	0.90 ± 0.10	29.16 ± 0.07	95%–99%
HCG-355	5	20 337.73	0.23 ± 0.03	28.55 ± 0.08	95%–99%
HII-357	6	18 317.17	2.00 ± 0.10	29.49 ± 0.04	≥99%
HII-357	3	15 805.94	2.60 ± 0.10	29.59 ± 0.04	≤90%
HII-357	2	8353.95	2.20 ± 0.20	29.52 ± 0.05	≥99%
HII-357	1	3776.86	3.90 ± 0.30	29.77 ± 0.06	≥99%
HCG-375	4	14 399.67	3.80 ± 0.20	29.76 ± 0.04	≤90%
HCG-394	5	21 263.52	0.27 ± 0.04	28.61 ± 0.08	≤90%
HCG-422	5	18 808.66	0.90 ± 0.10	29.14 ± 0.05	≥99%
HCG-428	5	12 795.41	1.20 ± 0.10	29.25 ± 0.06	≥99%
HII-451	6	24 854.78	0.80 ± 0.10	29.06 ± 0.05	≥99%
HII-624	6	23 881.36	0.53 ± 0.05	28.90 ± 0.06	95%–99%
HII-762	4	23 298.14	0.60 ± 0.10	28.96 ± 0.06	≤90%
HII-762	3	19 508.74	0.60 ± 0.10	28.99 ± 0.06	≥99%
HII-882	4	19 731.43	1.60 ± 0.10	29.40 ± 0.04	≤90%
HII-882	2	8797.02	1.90 ± 0.10	29.46 ± 0.05	90%–95%
HII-890	3	18 765.51	0.60 ± 0.10	28.97 ± 0.06	≤90%
HII-906	6	20 169.67	0.70 ± 0.10	29.05 ± 0.06	≤90%
HII-906	3	14 875.31	1.30 ± 0.10	29.28 ± 0.05	90%–95%
HII-930	4	24 319.02	0.70 ± 0.10	29.01 ± 0.05	≤90%
HII-930	3	20 323.13	0.50 ± 0.05	28.89 ± 0.06	≤90%
HII-930	2	11 149.19	0.60 ± 0.10	28.93 ± 0.08	≥99%
HII-1061	4	23 917.99	0.70 ± 0.10	29.04 ± 0.05	≤90%
HII-1061	2	11 098.91	0.90 ± 0.10	29.15 ± 0.06	≥99%
HII-1061	1	5308.81	0.90 ± 0.10	29.14 ± 0.08	≥99%
HII-1061	7	6713.37	0.80 ± 0.10	29.11 ± 0.08	≤90%
HII-1094	2	12 036.83	0.70 ± 0.10	29.05 ± 0.07	≥99%
HII-1094	4	25 843.12	0.60 ± 0.05	28.96 ± 0.06	≤90%
HII-1094	1	5205.37	1.30 ± 0.20	29.31 ± 0.07	≥99%
HII-1094	3	20 240.71	1.00 ± 0.10	29.18 ± 0.05	90%–95%
HII-1100	4	18 851.04	3.00 ± 0.10	29.66 ± 0.04	≥99%
HII-1100	3	20 552.09	4.50 ± 0.10	29.84 ± 0.03	≥99%
HII-1100	2	7614.88	2.10 ± 0.20	29.50 ± 0.05	≥99%

Table 3. continued.

Name	Obs. id.	Exposure Time (s)	Rate ± err. [10^{-2} cnt/s]	$\log L_x$ ± err. [erg/s]	CL range for variability
HII-1100	1	5138.86	1.50 ± 0.20	29.36 ± 0.07	≥99%
HII-1100	7	6244.38	2.50 ± 0.20	29.59 ± 0.05	≤90%
HII-1100	6	16 857.87	1.10 ± 0.10	29.22 ± 0.05	≤90%
HII-1103	4	21 374.72	0.70 ± 0.10	29.00 ± 0.06	≤90%
HII-1280	4	22 897.96	0.90 ± 0.10	29.15 ± 0.05	≤90%
HII-1280	3	18 107.51	1.50 ± 0.10	29.35 ± 0.05	95%–99%
HII-1280	7	6667.56	1.10 ± 0.10	29.21 ± 0.07	≤90%
HII-1286	4	24 786.47	0.48 ± 0.04	28.87 ± 0.06	≤90%
HII-1286	2	9267.3	0.60 ± 0.10	28.99 ± 0.08	≥99%
HII-1348	3	19 673.59	0.44 ± 0.05	28.83 ± 0.07	≥99%
HII-1348	1	4303.55	1.00 ± 0.20	29.17 ± 0.09	≥99%
HII-1355	4	22 626.35	1.60 ± 0.10	29.38 ± 0.04	≥99%
HII-1355	3	20 733.15	1.80 ± 0.10	29.43 ± 0.04	≤90%
HII-1355	2	11 293.6	1.20 ± 0.10	29.26 ± 0.06	≥99%
HII-1355	1	5339.06	0.90 ± 0.10	29.14 ± 0.08	≥99%
HII-1355	7	6335.15	1.70 ± 0.20	29.42 ± 0.06	≤90%
HII-1516	5	16 058.9	5.10 ± 0.20	29.89 ± 0.04	≥99%
HII-1516	4	20 158.86	1.70 ± 0.10	29.40 ± 0.04	90%–95%
HII-1516	3	19 887.06	1.60 ± 0.10	29.38 ± 0.04	95%–99%
HII-1516	1	4971.84	1.40 ± 0.20	29.32 ± 0.07	≥99%
HII-1516	7	6052.33	2.10 ± 0.20	29.51 ± 0.06	95%–99%
HII-1531	4	23 506.75	1.30 ± 0.10	29.30 ± 0.04	≤90%
HII-1531	3	19 465.06	1.30 ± 0.10	29.31 ± 0.05	≤90%
HII-1531	2	10 088.03	1.30 ± 0.10	29.28 ± 0.06	≥99%
HII-1531	1	4928.02	1.60 ± 0.20	29.38 ± 0.07	≥99%
HII-1531	7	5905.66	1.60 ± 0.20	29.39 ± 0.06	≤90%
HII-1532	4	23 213	1.40 ± 0.10	29.33 ± 0.04	≤90%
HII-1532	3	16 724.6	1.10 ± 0.10	29.24 ± 0.05	≤90%
HII-1532	2	9998.43	1.70 ± 0.10	29.42 ± 0.05	≥99%
HII-1653	5	14 717.69	1.90 ± 0.10	29.47 ± 0.05	≥99%
HII-1827	1	3770.5	1.50 ± 0.20	29.37 ± 0.08	≥99%
HII-2034	5	14 226.85	1.80 ± 0.10	29.45 ± 0.05	90%–95%
HII-2034	3	17 506.58	2.10 ± 0.10	29.50 ± 0.04	90%–95%
HII-2034	1	4234.99	1.60 ± 0.20	29.39 ± 0.07	≥99%
HII-2034	7	5227.81	1.40 ± 0.20	29.33 ± 0.07	95%–99%
HII-2208	5	15 768.04	1.00 ± 0.10	29.19 ± 0.05	≤90%
HII-2208	3	13 735.44	1.00 ± 0.10	29.19 ± 0.06	≥99%
HII-2244	5	16 402.28	4.10 ± 0.20	29.80 ± 0.04	≥99%
HII-2407	5	20 839.34	0.70 ± 0.10	29.01 ± 0.06	≤90%
HII-2548	5	20 056.96	0.42 ± 0.05	28.8 ± 0.07	≤90%
HII-2588	5	20 225.96	0.60 ± 0.10	28.97 ± 0.06	≤90%
HII-2601	5	21 673.56	0.90 ± 0.10	29.14 ± 0.05	90%–95%
HII-2741	5	19 687.32	1.20 ± 0.10	29.25 ± 0.05	≥99%
HII-3019	5	14 636.22	1.00 ± 0.10	29.18 ± 0.06	≤90%
HII-3096	5	17 848.54	2.80 ± 0.10	29.63 ± 0.04	≤90%
HII-3163	5	15 098.78	3.00 ± 0.10	29.67 ± 0.04	≤90%
HII-3197	5	15 434.75	6.70 ± 0.20	30.01 ± 0.03	≤90%
SK-586	6	25 530.99	0.38 ± 0.04	28.76 ± 0.06	≥99%

our sample stars in order to have a statistical evaluation of the X-ray variability. For each observation, we also ran the K-S test on the background counts to monitor possible background variability. Three cases in the dF7-dK2 sample have a variable background with Confidence Level (CL) > 99%: HII-1032 (Obs. seq. 200008a01), HII-727 (Obs. seq. 200008a01) and HII-1032 (Obs. seq. rp200068a00). Also four cases in the dK3-dM sample, have a background

variable with CL > 99%: HII-357 (Obs. seq. 200008a00), HII-1531 (Obs. seq. 200008a01), HII-1532 (Obs. seq. 200008a01) and HII-1355 (Obs. seq. 200068a00). However in all these cases the results of the test variability are nevertheless acceptable, since the background counts are much lower than those of the source.

Column 6 of the Tables 2 and 3 reports the CL at which we can reject the null hypothesis of the source being constant. Tables 4 summarize the K-S test results for dF7-dK2 and dK3-dM stars on short (hours) time scales; the percentage of cases of significant variability for both samples of dF7-dK2 and dK3-dM stars is of the same order. This result suggests that properties of the variability do not depend on the mass for the time scales and mass values explored. This finding is consistent with the hypothesis that the X-ray variability on short time scales (flare-like) is equally common among dF7-dK2 and dK3-dM stars.

3.2. Time X-ray distribution functions

We derived the Time Amplitude X-ray luminosity Distribution function (Time XAD) for both samples of dF7-dK2 and dK3-dM stars. Time XAD yields the fraction of time that a star spends with a flux higher, by a given factor, than its minimum value vs. the factor itself; this distribution is constructed by considering for each star the ratio between the observed L_x in each segment of an observation and the minimum L_x value in the same observation. It is therefore relative to a short time scale (hours). A more detailed account of Time XAD derivation is given in Paper I.

In Fig. 1 we show the Time XADs for dF7-dK2 and dK3-dM Pleiades stars yielding at least 500 counts. The two distributions show difference at all amplitudes: using the two sample K-S test, we tested the null hypothesis that the two distributions are drawn from the same parent distribution, finding that the two distributions are different. In particular, dK3-dM Pleiades stars are more variable than dF7-dK2 ones (CL ≥ 99%). Considering that an important contributor to the variations on short time scales are flares, this suggests that dK3-dM Pleiades stars have larger fractional variations than dF7-dK2 ones, probably due to flares. However, the frequency of variations in the two sets appears comparable as indicated by the K-S results (see Table 4).

3.3. X-ray variability on longer time scale

A subsample of our dF7-dK2 and dK3-dM Pleiades stars were multiply observed with a time separation of at least 15 days. In order to investigate the presence of medium – long time scale variations, we selected the observations with CL < 99%, in order to avoid any influence from short term variability. For these stars, we studied how the $< L_x >$ changes between different observations; in particular if L_1 and L_2 are the average X-ray luminosities of a star in two observations and δL_1 and δL_2 are the statistical errors of L_1 and L_2 respectively, we evaluated $\Delta L = |L_1 - L_2|$ and the statistical error $\delta L = \sqrt{(\delta L_1^2 + \delta L_2^2)}$. We
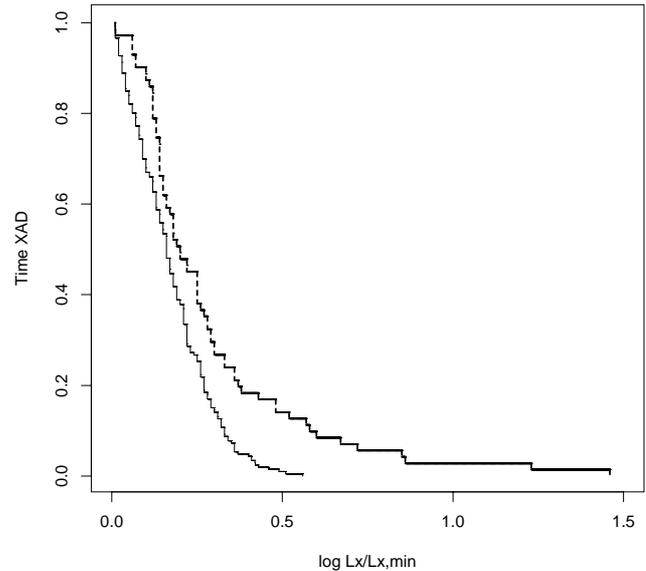

Fig. 1. The Time XAD for dF7-dK2 (thin line) and dK3-dM (thick line) Pleiades stars on short (hours) time scales, having at least 500 counts. The null hypothesis that that the two distributions are drawn from the same parent distribution can be rejected at a CL > 99%.

consider variable those stars for which $\frac{\Delta L}{\delta L} > 2$ corresponding to a 95.4.% confidence level.

Some stars show variability by a factor 2–3, on medium (15 d–1 yr) time scales (see Tables 5, 6) and variability is more common among the dF7-dK2 Pleiades stars than among the dK3-dM ones. Indeed, six out of eleven dF7-dK2 Pleiades stars have $\frac{\Delta L}{\delta L} > 2$ on time scales in the range (15 d–1 yr) while only three out of eleven dK3-dM stars are variable on the same time scale. We note that HII-1207 shows significant variations on a time scale comparable to its rotation period (15 days). Much longer time scales (6–12 months) are involved for the others stars. This suggests that variations on medium or long time scales possibly due to rotational modulation and/or cyclic behavior are present in dF7-dK2 Pleiades stars. We note that one of the three variable dK3-dM stars (HII-906) shows $\frac{\Delta L}{\delta L} = 2.92$ while the other two (HII-1100 and HII-2034) have spectral type K3 and K2.5 respectively, and likely are more similar to the dF7-dK2 sample, reinforcing that long term variations can be common among solar-like type stars and less common among low mass stars.

3.4. Age effect: Comparison with late-type field stars

A number of studies on open clusters and field stars samples (e.g. Caillault & Helfand 1985; Micela et al. 1985, 1990, 1996; Stern et al. 1981; Micela et al. 1988; Maggio et al. 1987; Barbera et al. 1993; Stauffer et al. 1994) have established the decrease of X-ray emission level with increasing age as an effect of rotational braking; in particular the median of L_x decreases by three dex with a spread of ~1 dex. It is not clear how much of this spread is due to variability and if and how variability properties change with age.

We compared the Time XAD for dF7-dK2 and dK3-dM Pleiades stars with the analogous ones obtained for dF7-dK2

Table 4. Results of the K-S test on short time scales for dF7-dK2 and dK3-dM Pleiades stars (% and numbers).

CL range for variability	Number of dF7-dK2 observations	Number of dK3-dM observations
>99%	**38% (34)**	**43% (46)**
95%–99%	9% (8)	9% (10)
90%–95%	8% (7)	7% (8)
≤90%	**45% (40)**	**41% (44)**

Table 5. Variability on longer time scale: here we use multiple ROSAT observations of dF7-dK2 Pleiades stars separed by at least 0.5 months.

Name	$< L_x >$ range [erg/s]	$\frac{\Delta L}{\delta L}$ on medium-time scale	Elapsed time of each obs. [hours]	Time between obs. [months]
HII-253	29.87–30.11	4.44	1.16–3.62	12
HII-708	29.63–28.82	6.02	1.18–4.51	12
HII-727	29.75–29.83	<2	1.35–4.14	12
HII-738	29.58–29.70	<2	1.29–6.54	12
HII-761	29.62–29.73	<2	5.09–5.15	0.5
HII-1032	29.96–29.99	<2	1.48–4.91	12
HII-1124	29.29–29.30	<2	1.80–6.95	12
HII-1136	29.54–29.78	3.49	1.19–6.06	12
HII-1207	28.97–29.47	6.50	4.12–5.00	0.5
HII-1726	29.23–29.46	2.67	1.18–4.84	12
HII-1856	29.18–29.43	3.63	2.74–5.83	6

Table 6. As in Table 5 for dK3-dM Pleiades stars.

Name	$< L_x >$ range [erg/s]	$\frac{\Delta L}{\delta L}$ on medium-time scale	Elapsed time of each obs. [hours]	Time between obs. [months]
HCG-244	28.87–29.02	<2	1.85–6.05	12
HCG-277	29.02–29.16	<2	2.63–6.83	6
HII-882	29.40–29.46	<2	2.44–5.48	6
HII-906	29.05–29.28	2.92	4.13–5.60	0.5
HII-1061	29.04–29.11	<2	1.86–4.44	12
HII-1100	29.22–29.59	4.58	1.73–4.68	12
HII-1280	29.15–29.21	<2	1.85–6.36	12
HII-1355	29.42–29.43	<2	1.76–5.76	12
HII-1516	29.38–29.51	<2	5.52–5.60	12
HII-1531	29.30–29.39	<2	1.64–6.53	12
HII-2034	29.33–29.50	2.27	1.45–4.86	12

field stars (Paper II) and dK3-dM field stars (Paper I), on short time scales. For the comparison we used only the stars with at least 500 counts in order to avoid a possible bias due to the different statistics.

In Fig. 2 we show the Time XAD for dF7-dK2 Pleiades stars and dF7-dK2 field stars; the distributions are significantly different at all amplitudes. Since we have compared two samples including stars of different L_x levels, it remains unclear if the difference we found is due to the different ages or to the different average L_x of the two samples. In order to investigate this issue we have repeated our analysis by considering two subsamples of Pleiades and field stars of similar activity level, as characterized by the L_x, in the range 29.45–30.25. The null hypothesis that these two subsamples are drawn from the same parent distribution can be rejected at only a confidence level ≥26%; this result indicates that the variability amplitudes are indeed related to L_x and not to stellar age.

The comparison between the Time XADs of dK3-dM Pleiades stars and dK3-dM field stars (Paper I) is shown in Fig. 3. In this case we do not find indications of strong differences, independent of L_x ranges, confirming the result in
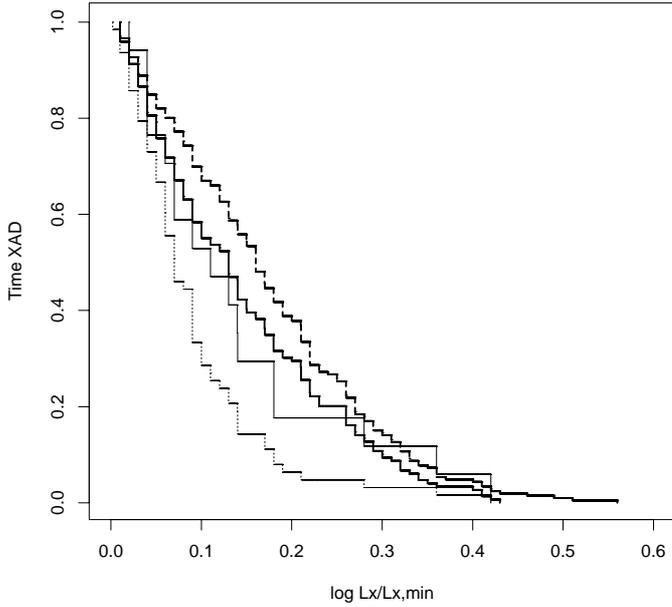
Fig. 2. The Time XAD for dF7-dK2 field (thin dotted line) and dF7-dK2 Pleiades stars (thick dashed line), having at least 500 counts. We also show the Time XAD for dF7-dK2 Pleiades stars (thick line) and dF7-dK2 field stars (thin line) with more than 500 counts and in the same range of $< L_x >$.

Fig. 3. The Time XAD for dK3-dM field (thick line) and dK3-dM Pleiades (thin line) stars on short time scales, having at least 500 counts. The probability that the two samples came from the same parent distribution is >99%.

Paper I that the amplitude of variability of low mass stars does not change with L_x or age.

4. Summary and conclusions

We analyzed the characteristics of the X-ray variability of dF7-dK2 and dK3-dM stars in the Pleiades cluster, observed with ROSAT-PSPC. Using all the observations of ROSAT-PSPC, we explored X-ray variability on short (hours) and medium (months) time scales. The samples includes 89 observations of 42 distinct dF7-dK2 Pleiades stars, and 108 observations of 61 dK3-dM Pleiades stars. Applying the unbinned Kolmogorov-Smirnov test on all the X-ray photon time series of our samples we find that the percentage of variable stars in dF7-dK2 and dK3-dM stars is quite similar, suggesting that, on short time scales, the X-ray variability does not depend on mass.

For our samples, we computed the Time distribution function of the X-ray Amplitude variations, that yields the fraction of time that a star spends with a flux higher by a certain factor than its minimum value. Our results are in agreement with Gagné et al. (1995) who find ~25% of the late-type Pleiades stars variable by more than a factor of two.

The analysis of a few stars observed on medium time scales (15 d–1 yr) shows that the dF7-dK2 Pleiades stars are variable on medium or long time scales, while dK3-dM Pleiades stars are not. This result suggests that rotational modulation and/or cyclic behavior may be present in dF7-dK2 Pleiades stars, but not in dK3-dM stars and that the variability observed on medium and short time scales may have a different physical origin. We note that most of the few dK3-dM stars in the Ca II H and K Mount Wilson sample do show cyclic light
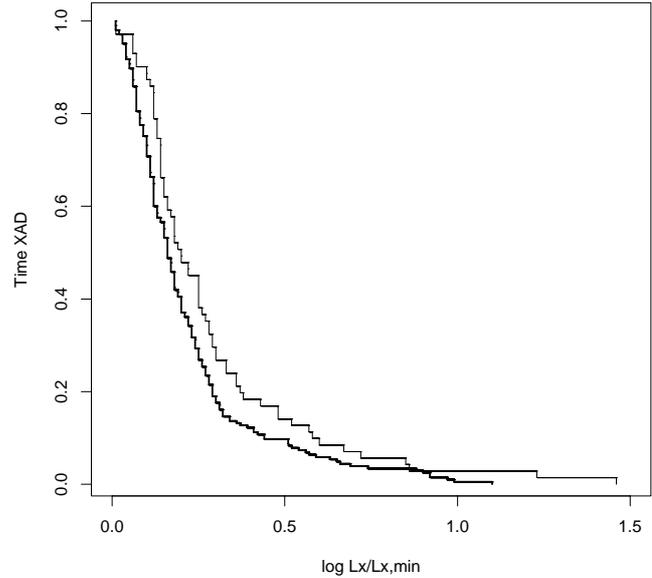
curves (see Fig. 2, Baliunas et al. 1995). We cannot exclude that a cyclic behavior is present in the X-ray emission of dK3-dM Pleiades stars, but if long term variations exist, they must be of much smaller amplitudes than the short term variations which dominate the ROSAT X-ray light curves.

We compared the Time XADs of dF7-dK2 and dK3-dM Pleiades stars with the corresponding distributions of dF7-dK2 and dK3-dM field stars. It appears that the variations on short time scales for dF7-dK2 samples strongly depend on L_x but not on stellar age.

On short time scales the dK3-dM Pleiades stars are very similar to dK3-dM field stars, suggesting that, for low mass stars, the amplitude of variability does not change with L_x or age.

References

Barbera, M., Micela, G., Sciortino, S., Harnden, F. R., & Rosner, R. 1993, ApJ, 414, 846

Bohlin, R. C., Savage, B. D., & Drake, J. F. 1978, ApJ, 224, 132

Caillault, J.-P., & Helfand, D. J. 1985, ApJ, 289, 279

Daniel, K. J., Linsky, J. L., & Gagné, M. 2002, ApJ, 578, 486

Eadie, W. T., Drijard, D., & James, F. E. 1971, Statistical methods in experimental physics (Amsterdam: North-Holland)

Gagné, M., Caillault, J., & Stauffer, J. R. 1995, ApJ, 450, 217

Kahler, S. W., & Kreplin, R. W. 1991, Sol. Phys., 133, 371

Kreplin, R. W., Dere, K. P., M., H. D., & Meekins, J. F. 1977, The solar output and its variations (Colorado University press), 187

Krishnamurthi, A., Reynolds, C. S., Linsky, J. L., Martín, E., & Gagné, M. 2001, AJ, 121, 337

Maggio, A., Sciortino, S., Vaiana, G. S., et al. 1987, ApJ, 315, 687

Marino, A., Micela, G., & Peres, G. 2000, A&A, 353, 177

Marino, A., Micela, G., Peres, G., & Sciortino, S. 2002, A&A, 383, 210

Mermilliod, J.-C., Turon, C., Robichon, N., Arenou, F., & Lebreton, Y. 1997, in ESA SP-402: Hipparcos – Venice '97, 402, 643

Micela, G., Sciortino, S., Harnden, F. R., et al. 1999, A&A, 341, 751

Micela, G., Sciortino, S., Kashyap, V., et al. 1996, ApJS, 102, 75

Micela, G., Sciortino, S., Serio, S., et al. 1985, ApJ, 292, 172

Micela, G., Sciortino, S., Vaiana, G. S., Harnden, F. R., Rosner, R., & Schmitt, J. H. M. M. 1990, ApJ, 348, 557

Micela, G., Sciortino, S., Vaiana, G. S., et al. 1988, ApJ, 325, 798

Orlando, S., Peres, G., & Reale, F. 2001, ApJ, 560, 499

Peres, G., Orlando, S., Reale, F., Rosner, R., & Hudson, H. 2000, ApJ, 528, 537

Schmitt, J. H. M. M., Kahabka, P., Stauffer, J., & Piters, A. J. M. 1993, A&A, 277, 114

Siegel, S. 1956, Nonparametric statistics for the behavioral sciences, International Student Edition – McGraw-Hill Ser. in Psychology (Tokyo: McGraw-Hill Kogakusha)

Stauffer, J. R., Caillault, J.-P., Gagne, M., Prosser, C. F., & Hartmann, L. W. 1994, ApJS, 91, 625

Stern, R. A., Zolcinski, M. C., Antiochos, S. K., & Underwood, J. H. 1981, ApJ, 249, 647

Vaiana, G., & Tucker, W. H. 1974, in X-ray Astronomy, ASSL, 43, 169

Vaiana, G. S., Davis, J. M., Giacconi, R., et al. 1973, ApJ, 185, L47

Withbroe, G. L., Habbal, S. R., & Ronan, R. 1985, Sol. Phys., 95, 297